

PACS numbers: 62.23.Pq, 71.20.Nr, 73.50.Lw

## ENHANCEMENT IN THERMOELECTRIC POWER IN LEAD TELLURIDE NANOCOMPOSITE: ROLE OF OXYGEN VIS-A-VIS NANOSTRUCT.

**B. Paul, P. Banerji**

Materials Science Centre  
Indian Institute of Technology, Kharagpur 721302, India  
E-mail: [biplabpaul2006@yahoo.co.in](mailto:biplabpaul2006@yahoo.co.in)

*The present work reports enhanced power factor and reduced value of room temperature thermal conductivity in undoped PbTe nanocomposite, prepared from PbTe nanocrystals, synthesized via chemical route. The highest power factor is found to be  $19.21 \times 10^{-4} \text{ Wm}^{-1}\text{K}^{-2}$  with room temperature thermal conductivity of  $1.53 \text{ Wm}^{-1}\text{K}^{-1}$ . The potential barrier at the sharp interfaces of the grains of the nanocomposites, occurred due to the adsorption of oxygen by the grain surfaces, have been found to play the main role to produce the high value of Seebeck coefficient ( $416 \mu\text{V/K}$  at 500 K) by preferentially scattering the lower energy electrons and thus enhancing the power factor. The lattice destruction at the grain interfaces has been found to cause the remarkable reduction in thermal conductivity, through scattering a wide spectrum of phonon wavelength.*

**Keywords:** LEAD TELLURIDE, HOT-PRESS, NANOCOMPOSITE, THERMOELECTRIC, ENERGY FILTERING.

(Received 04 February 2011, in final form 13 October 2011)

### 1. INTRODUCTION

Thermoelectric efficiency of any thermoelectric material is expressed in terms of a factor, thermoelectric figure of merit,  $Z_T = \alpha^2 \sigma T / k$ , where  $\alpha$  is the Seebeck coefficient,  $\sigma$  is the electrical conductivity,  $T$  is the absolute temperature and  $k$  is the thermal conductivity, respectively. To enhance  $Z_T$  of a thermoelectric system power factor ( $\text{PF} = \alpha^2 \sigma$ ) must have to be enhanced together with a simultaneous reduction in  $k$ . For a three dimensional system,  $\alpha$  is inversely related with  $\sigma$  according as,

$$\alpha = \frac{\pi^2}{3} \frac{k_B^2 T}{e} \left. \frac{d \ln \sigma(E)}{dE} \right|_{E=E_F}, \quad (1)$$

where  $k_B$  is the Boltzmann constant,  $e$  is the electronic charge and  $E_F$  is the Fermi energy. The above equation predicts that an enhancement in  $\alpha$  must be accompanied with the simultaneous reduction in  $\sigma$ . So, it is challenging, for a thermoelectric system, to enhance  $\alpha$  without affecting  $\sigma$ . To tackle this difficulty researchers have developed many strategies, e.g. (I) carrier pocket engineering [1], (II) local distortion of the band [2], (III) semimetal to semiconductor transition [3], (III) quantum confinement [4, 5]. Among all the strategies, we have implemented here the concept of energy filtering of carriers to enhance the power factor of the thermoelectric specimens. Besides, here we have tried to reduce lattice thermal conductivity by the

introduction of size effect on phonon by reducing structural characteristic length of the system. For the purpose, we have prepared the samples by compaction of PbTe nanoparticles, synthesized via solution phase chemical synthesis, under high pressure and temperature. Compaction of nanoparticles under high pressure and temperature enable us to introduce a large number of interfaces within the matrix of PbTe nanocomposites. The potential barrier developed at the grain interfaces scatter lower energy charge carriers enhancing its average energy, which in effect causes an enhancement in  $\alpha$ . Further, the large number of interfaces causes an enhancement of phonon scattering, which results in a dramatic reduction in phonon thermal conductivity of the materials. The thermoelectric parameters of the nanocomposites have been compared with the results that obtained from a bulk p-type PbTe grown by Bridgman method. The possible mechanisms involved in the reduction in thermal conductivity of nanocomposites have been discussed here on the basis of both the particle and wave aspects of phonon.

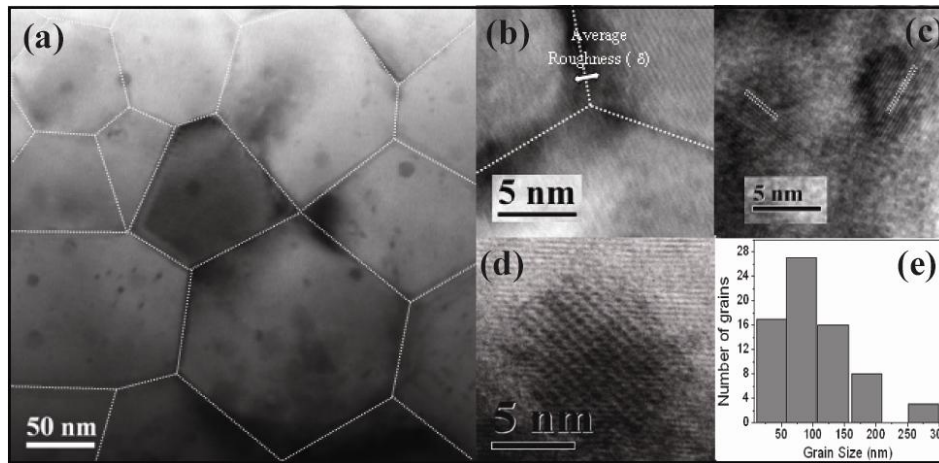
## 2. EXPERIMENTAL

For the preparation of the PbTe nanocomposites the nanoparticles synthesized by the process described elsewhere [6]. The nanoparticles were compacted under the pressure of 250 MPa at temperature 850 K under argon atmosphere. The pellets of diameter 12 mm and of thickness 2 mm were obtained. The density of the obtained pellets was determined by Archimedes method and found to be  $\sim 98\%$ . Bulk undoped p-type PbTe was grown by Bridgman method as described elsewhere [7]. Thermal conductivity of the specimens was measured by parallel heat conductance method as described elsewhere [8].

## 3. RESULTS AND DISCUSSION

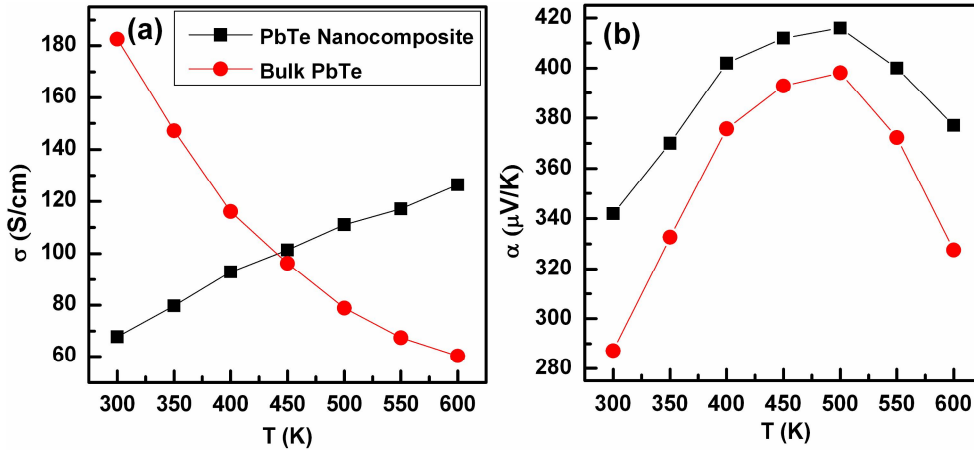
By X-ray diffraction spectra analysis, apart from the peaks of cubic phase of PbTe rock salt crystal structural the presence of few impurity peaks of  $\text{PbTeO}_3$  of very small intensities have been confirmed. Also, EDS analyses reveal the presence of nearly 2-3 at. % of oxygen in the samples.

Fig. 1(a) shows the transmission electron microscopic image (TEM) of PbTe nanocomposite specimen, which reveals the presence of grains with a certain distribution in size in the range of 25-350 nm. Usually, the grains are polygonal as observed in Fig. 1(a). Selected area electron diffraction shows that the grains are single crystals with random orientations. Fig. 1(e) shows the grain size distribution. From TEM image analyses it is found that that nearly 80 % of the grains are smaller than 150 nm in size and shown by the grain size distribution curve Fig. 1(e). Nearly 40 % of the total grains fall into the range of 50-100 nm. In addition to the nanometer dimensional grains there are many nanoprecipitates, which are embedded in the grains. Fig. 1(b) shows the high-resolution TEM (HRTEM) image of grain boundaries between three adjacent grains. In spite of the fact that from Fig. 1(a) it may seem that grain boundaries are clean and sharp, HRTEM image analysis shows a roughness of nearly thrice of the distance between the nearest atoms in PbTe crystal lattice (as shown in Fig. 1(b)). Two types of nanodots have been found to be embedded within the grains. Fig. 1(c) shows the nanodots with twisted boundaries with similar chemical composition as that of surrounding matrix, as confirmed by energy dispersive spectrum (EDS) analyses. On the other hand Fig. 1(d) shows Pb-rich nanodots, as confirmed by EDS analyses, which remains endotaxially embedded within the matrix.



**Fig. 1** – (a) A typical TEM image of multigrains of PbTe nanocomposite specimen, (b) HRTEM image of adjacent three grains showing the roughness of the grain interfaces, (c) precipitate with twisted boundaries but with similar chemical composition as the surrounding matrix. (d) Pb-rich nanoprecipitate, (e) grain size distribution

The room temperature hole concentration of bulk and PbTe nanocomposite specimen has been found to be  $1.492 \times 10^{18}$  and  $1.57 \times 10^{18} \text{ cm}^{-3}$ , respectively. It is found that the presence of excess Pb in undoped PbTe causes the n-type conductivity [9]. However, Hall measurements confirm the p-type conductivity of PbTe nanocomposite specimen. The adsorption of oxygen by the grain surface during hot pressing causes an inversion of electrical conductivity of the specimen from n-type to p-type. The adsorbed oxygen at the grain surface draws electrons from within the grains and creates acceptor states at the boundaries [10]. So, while passing through the boundaries electrons get trapped by these acceptor states and forms potential barrier ( $E_b$ ) across the grain interfaces [11]. At room temperature, the electrical conductivity of the nanocomposite and bulk PbTe specimens are 67.84 and 182.62 S/cm, respectively. The electrical conductivity of nanocomposite increases with the increase in temperature as shown in Fig. 2(a), which is opposite in nature as compared to that of bulk PbTe crystal. This opposite nature of temperature dependency of electrical conductivity of the nanocomposite specimen is attributed to the potential barrier scattering of the carriers at the grain interfaces. The potential energy barrier ( $E_b$ ) at the grain boundaries related with the electrical conductivity of the specimen according as  $\sigma \sim \exp(-E_b/k_B T)$  [12]. At low temperature, all the carriers do not gain sufficient thermal energy to overcome the potential barrier across the grain boundaries to take part in transport process and thus electrical conductivity remains low. However, with the increase of temperature number of carriers, which acquires sufficient energy to cross that barrier increases enhancing electrical conductivity of the specimen. So, with the increase of temperature the electrical conductivity of the specimen increases.



**Fig. 2** – Temperature dependent (a) electrical conductivity and (b) Seebeck coefficient of the nanocomposite and bulk PbTe in the temperature range 300-600 K

Fig. 2(b) shows the temperature dependent Seebeck coefficient of the nanocomposite and bulk PbTe in the range 300-600 K. At room temperature, the value of Seebeck coefficient of nanocomposite specimen is  $342 \mu\text{V/K}$ , which is higher than the value obtained for bulk PbTe ( $287 \mu\text{V/K}$ ). The Seebeck coefficient of both the specimens increases with temperature and attains a maximum value at a certain temperature beyond which Seebeck coefficient again begins to fall with the further increase in temperature. The maximum obtained value of Seebeck coefficient of nanocomposite has been found to be  $416 \mu\text{V/K}$  at 500 K. It has been found that lower energy carriers have a negative contribution to the Seebeck coefficient [13]. At the inter-grain regions scattering of the lower energy carriers being high the Seebeck coefficient at this region, denoted by  $\alpha_b$ , becomes higher than the Seebeck coefficient at the grain regions and which is denoted here by  $\alpha_g$  [14, 15]. The total Seebeck coefficient of the nanocomposite specimen can be expressed as [14, 15],

$$S_g = S_g + (S_b - S_g) \times (l_c/d) \quad (2)$$

Here,  $l_c$  is the mean free path of the carriers, and  $d$  is the size of the grains. In nanocomposite specimen, due to its small grain size, the volume fraction of the intergrain regions increases enhancing its contribution to the Seebeck coefficient. In our samples, average grain size is smaller and corresponding volume fraction of intergrain regions higher than the samples prepared by the investigators reported elsewhere [16, 17]. Thus the Seebeck coefficient of the present samples becomes higher than the values reported for the undoped PbTe nanocomposites. With the increase in temperature the average energy of the carriers increases, which results in an enhancement of the Seebeck coefficient of the both the nanocomposites and bulk specimens. However, beyond a certain temperature the number electron and hole pairs increases, which causes a reduction in the value of Seebeck coefficient of the specimens with temperature. Fig. 3 shows the temperature dependent power factor of both the specimens in the temperature range 300-600 K. At room

temperature, the power factor of nanocomposite and bulk specimens are  $7.93 \times 10^{-4}$  and  $15.06 \times 10^{-4} \text{ Wm}^{-1}\text{K}^{-2}$ , respectively. Although, at room temperature, the power factor of the nanocomposite specimens remains low its power factor attains a value of  $19.21 \times 10^{-4} \text{ Wm}^{-1}\text{K}^{-2}$  at  $T = 500 \text{ K}$ , which is considerably higher than that of bulk PbTe [18, 19]. That enhancement of power factor in nanocomposite specimens occurred due to the simultaneous enhancement of both the electrical conductivity and Seebeck coefficient with temperature.

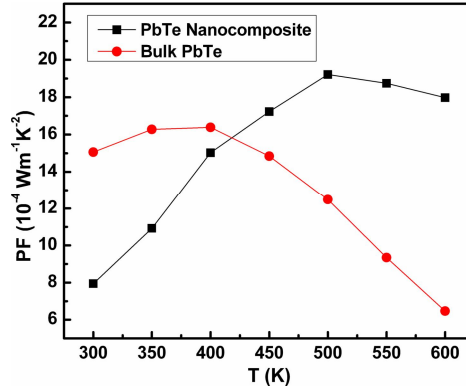


Fig. 3 – Temperature dependent power factor of the nanocomposite and bulk PbTe in the temperature range 300-600 K

At room temperature, thermal conductivity of the nanocomposite specimen is found to be  $1.53 \text{ Wm}^{-1}\text{K}^{-1}$ , which is considerably low as compared to the typical value of  $2.3 \text{ Wm}^{-1}\text{K}^{-1}$  as reported for p-type bulk PbTe. The reduction in thermal conductivity of any materials without affecting its electrical conductivity is very challenging part in thermoelectricity. Though the roughness ( $\delta$ ) of 3-4 atomic layers at the grain boundaries, as shown in Fig. 1(b), do not cause much reduction in electrical conductivity, it is sufficient to reduce thermal conductivity of the nanocomposite specimens remarkably through the destruction of the coherency of the phonon wave. It has been found that for phonon of wavelength  $\lambda$  the interface can be considered as smooth or rough according as [20],

$$\frac{\delta}{\lambda} \begin{cases} \gg 0.1 \text{ (Rough)} \\ \ll 0.1 \text{ (Smooth)} \end{cases} \quad (3)$$

Taking the longitudinal sound velocity ( $v_l$ ) as 1730 m/s [21] we obtained the average phonon wavelength as 1.66 nm at  $T = 300 \text{ K}$  from the relation  $\lambda = 2h v_l / k_B T$ . Here,  $k_B T / 2$  is the average thermal energy of the system,  $h$  is the Planck constant. So, at room temperature, the ratio  $\delta / \lambda \gg 0.1$ , i.e. the interfaces are sufficiently rough for phonon to be scattered. So far, we have treated phonon as wave to explain the possible reason of lower thermal conductivity of the nanocomposite specimen. However, wave property of phonon hold good when the structural characteristic length of the system becomes smaller than the coherence length of the phonon. Since, above room temperature, inelastic scattering of phonon becomes dominant, the phonon

coherence length can be assumed to be nearly equal to the mean free path of phonon. The phonon mean free path is found to be somewhere within the range 277-436 nm for PbTe [22]. But, about 80 % of the grains in our nanocomposite specimens are below 150 nm. Hence, size effect is introduced here, which tunes the phonon contribution to thermal conductivity. But still here the wave nature of the phonon cannot be restored, because of certain roughness of grain interfaces the interface scattering become diffusive. Thus, here the size effect, induced by the grains with size smaller than the phonon mean free path falls into classical regime, i.e. particle nature of phonon is dominant here. Because of larger phonon mean free path as compared to that of grain size the scattering rate of phonon increases, which results in much reduction in thermal conductivity of the system. So, both for the wave and particle aspects of phonon the interfacial scattering is an important factor for the reduction in thermal conductivity. It has been found that interfacial scattering does not depend on the periodicity and geometry of the grains; it only depends on the interface density (interfacial area per unit volume) of the nanocomposite specimen [23]. The interface density, in nanocomposite being higher its thermal conductivity is expected to be much reduced than that of its bulk counterpart as confirmed in our investigations. Further, the nanoprecipitates of dimension nearly 3-5 nm, as observed in our HRTEM image analyses is useful to scatter the short wavelength phonon, which is beneficial for the reduction in thermal conductivity of the specimen. So, due to enhanced power factor and reduced thermal conductivity PbTe nanocomposite specimen has higher thermoelectric efficiency than that of its bulk counterpart.

#### 4. CONCLUSION

In conclusion, hot-press method is found to be useful and simple way to incorporate large no of grains of nanodimensions within the matrix of PbTe. The potential energy barriers at the interfaces of the grains have been found to cause an enhancement of Seebeck coefficient of the nanocomposite specimens through preferential scattering of low energy electrons and reduction in thermal conductivity through destructive scattering of phonons. Due to its sharp grain interfaces the electrical conductivity of the nanocomposite specimens does not get much reduced. Hence, the remarkable enhancement of the Seebeck coefficient of the nanocomposite specimens causes a significant increase in its power factor as compared to that of bulk PbTe. Because of higher power factor and reduced thermal conductivity PbTe nanocomposite is found to be a potential candidate for thermoelectric applications.

The authors acknowledge technical support from Mr. R. Mukherjee and Mr. P. Chakroborty. One of the authors (BP) acknowledges financial support from UGC through UGC (NET).

#### REFERENCES

1. T. Koga, S.B. Cronin, M.S. Dresselhaus, *Appl. Phys. Lett.* **77**, 1490 (2000).
2. J.P. Heremans, V. Jovovic, E.S. Toberer, A. Saramat, K. Kurosaki, A. Charoenphakdee, S. Yamanaka, G.J. Snyder, *Science* **321**, 554 (2008).
3. L.D. Hicks, T.C. Harman, M.S. Dresselhaus, *Appl. Phys. Lett.* **63**, 3230 (1993).
4. L.D. Hicks, T.C. Harman, X. Sun, M.S. Dresselhaus, *Phys. Rev. B* **53**, R10493 (1996).

5. Y.M. Lin, S.B. Cronin, J.Y. Ying, M.S. Dresselhaus, J.P. Heremans, *Appl. Phys. Lett.* **76**, 3944 (2000).
6. B. Paul, P. Banerji, *Adv. Mat. Res.* **67**, 251 (2009).
7. B. Paul, P. Banerji, *J. Crystal Growth* **311**, 1260 (2009).
8. T. Dasgupta, A.M. Umarji, *Rev. Sci. Instrum.* **76**, 094901 (2005)
9. Z.H. Dughaish, *Physica B* **322**, 205 (2002).
10. E.I. Rogacheva, I.M. Krivulkin, O.N. Naschekina, A.Y. Sipatov, V.V. Volovuev, M.S. Dresselhaus, *Appl. Phys. Lett.* **78**, 1661 (2001).
11. J. Martin, L. Wang, L. Chen, G.S. Nolas, *Phys. Rev. B* **79**, 115311 (2009).
12. J.Y.W. Seto, *J. Appl. Phys.* **46**, 5247 (1975).
13. A.J. Minnich, M.S. Dresselhaus, Z.F. Ren, G. Chen, *Energy Environ. Sci.* **2**, 466 (2009).
14. K. Kishimoto, T. Koyanagi, *J. Appl. Phys.* **92**, 2544 (2002).
15. G.H. Blount, R.H. Bube, A.L. Robinson, *J. Appl. Phys.* **41**, 2190 (1970).
16. J. Martin, G.S. Nolas, W. Zhang, L. Chen, *Appl. Phys. Lett.* **90**, 222112 (2007).
17. B. Paul, P. Banerji, *Nanosci. Nanotechnol. Lett.* **1**, 208 (2009).
18. J.P. Heremans, C.M. Thrush, D.T. Moreli, *J. Appl. Phys.* **98**, 063703 (2005).
19. H. Wang, J.F. Li, T. Kita, *J. Phys. D: Appl. Phys.* **40**, 6839 (2007).
20. G. Chen, D.B. Tasciuc, R.G. Yang, *Encyclopedia of Nanoscience and Nanotechnology*, ed. H. S. Nalwa, Vol. 7 (American Scientific Publishers, Stevenson Ranch, 2004), pp. 429-459.
21. D.M. Rowe, C.M. Bhandari, *Modern Thermoelectrics* (Holt Saunders, London, 1983).
22. J.W. Roh, S.Y. Jang, J. Kang, S. Lee, J.S. Noh, W. Kim, J. Park, W. Lee, *Appl. Phys. Lett.* **96**, 103101 (2010).
23. M.S. Jeng, R. Yang, D. Song, G. Chen, *J. Heat Transfer* **130**, 042410 (2008).